The Palaeo-bathymetry of Base Aptian Salt Deposition on the Northern Angolan Rifted Margin: Constraints from Flexural Backstripping and Reverse Post-breakup Thermal Subsidence Modelling

L. Cowie[1], R. M. Angelo[1, 2], N. J. Kusznir[1] & G. Manatschal[3]

[1] Department of Earth & Ocean Sciences, University of Liverpool, Liverpool, L69 3BX, UK

[2] Presently at ConocoPhillips, Houston, TX 77079, USA

[3] CNRS-EOST, Université de Strasbourg, 1 rue Blessing, F-67084 Strasbourg, France

Abstract

The bathymetric datum with respect to global sea level for Aptian salt deposition in the South Atlantic is hotly debated. Some models propose that the salt was deposited in an isolated ocean basin in which local sea level was between 2km and 3km below the global level. In this study, we use reverse post-breakup subsidence modelling to determine the palaeo-bathymetry of base Aptian salt deposition on the Angolan rifted continental margin. The reverse post-breakup subsidence modelling consists of the sequential flexural isostatic backstripping of the post-breakup sedimentary sequences, decompaction of remaining sedimentary units and reverse modelling of post-breakup lithosphere thermal subsidence. The reverse modelling of post-breakup lithosphere thermal subsidence is carried out in 2D and requires knowledge of the continental lithosphere stretching factor (β), which is determined from gravity anomaly inversion. The analysis has been applied to the ION-GXT CS1-2400 deep long-offset seismic reflection profile and the P3 and P7+11 seismic cross sections of Moulin (2005) and Contrucci et al. (2004) offshore northern Angola. Reverse post-

breakup subsidence modelling restores the proximal autochthonous base salt to 200-300m below global sea level at the time of breakup. In contrast, the predicted water-loaded bathymetries of the more distal base salt restored to breakup time are much greater, ranging between 1km and 3km. The predicted bathymetries of the first unequivocal oceanic crust at breakup are approximately 2.5km, as expected for newly formed oceanic crust of 'normal' thickness. Several interpretations of these results are possible. Our preferred interpretation is that all Aptian salt on the northern Angola rifted continental margin was deposited 200-300m beneath global sea level and that the proximal salt subsided by post-rift (post-tectonic) thermal subsidence alone, while the distal salt formed during late syn-rift when the underlying crust was actively thinning resulting in additional tectonic subsidence (followed by post-rift thermal subsidence). An alternative interpretation is that the distal salt is para-autochthonous and moved down-slope into much deeper water during and just after breakup. We do not believe that a deep isolated ocean basin, with local sea level 2-3km beneath global sea level as has been proposed, is required to explain the Aptian salt deposition on the northern Angolan rifted continental margin.

Introduction

The northern Angolan rifted continental margin has been the subject of extensive seismic surveys (Contrucci et al., 2004; Moulin et al., 2005), due to its hydrocarbon resources. The presence of thick sedimentary packages impacted by a massive middle to upper Aptian salt sequence (up to 5km thickness in places), makes seismic imaging and interpretation of the sub-salt difficult and presents major scientific and technical challenges to understanding crustal structure and tectonic history. Whether the northern Angolan Aptian salt sequence is pre-breakup or post-breakup remains a topic of major debate; also the palaeo-water depths through the breakup period and the mechanisms responsible for generating accommodation space through time are uncertain (Jackson et al., 2000; Karner and Driscoll, 1999; Karner et al., 2003; Karner et al., 1997; Moulin, 2003; Moulin et al., 2005).

There is also much debate concerning the geometry and nature of the pre-salt basin, and the underlying crustal basement structure (Contrucci et al., 2004; Karner and Gambôa, 2007; Nurullina, 2006). Our analysis of the offshore northern Angolan margin is focussed on three profiles in the Kwanza region; locations are indicated in Figure 1(a). The three profiles include the ION-GXT deep long offset seismic reflection profile CS1-2400 (Figure 1(c)) and the P3 (Figure 1(d)) and P7+11 profiles (Figure 1(e)) (Contrucci et al., 2004; Moulin et al., 2005). The purpose of this paper is to provide an understanding of the palaeo-bathymetries of the base Aptian salt deposition (both proximal and distal) along the northern Angolan rifted continental margin and to understand how the salt sits within the broad framework of the ocean continent transition (OCT).

Reverse post-breakup thermal subsidence modelling

Reconstructed palaeo-bathymetries of base Loeme salt (top Aptian) along the CS1-2400, P3 and P7+11 profiles has been determined using reverse post-breakup subsidence modelling (Kusznir et al., 1995; Roberts et al., 1998). The reverse post-breakup subsidence modelling (Figure 2) consists of the sequential flexural isostatic backstripping of the post-breakup sedimentary sequences, decompaction of the remaining sedimentary units and reverse modelling of post-breakup lithosphere thermal subsidence. The magnitude of reverse post-breakup thermal subsidence is controlled by the continental lithosphere stretching factor (β) (McKenzie, 1978) which we predict from gravity anomaly inversion. The magnitude of β therefore controls the restored model elevation relative to sea level and the predicted palaeo-bathymetry (Roberts et al., 2009; Roberts et al., 1998). We use the CS1-2400 profile to describe in detail the modelling approach.

Continental lithosphere stretching factors (β) (McKenzie, 1978) range between one and infinity; for presentation purposes we prefer to use the related parameter, continental lithosphere thinning factor ($\gamma = 1-1/\beta$), which ranges between zero and one.

Our gravity anomaly inversion, uses bathymetry (Amante and Eakins, 2009) (Figure 1(a)), satellite derived free air gravity (Sandwell and Smith, 2009) (Figure 1(b)), sediment thickness data from the ION-GXT profile (Figure 1(c) and ocean age isochrons (Müller et al., 1997) to determine continental lithosphere thinning, crustal basement thickness and Moho depth. The gravity anomaly inversion is carried out in the 3D spectral domain using the scheme of Parker (1972) and also incorporates a lithosphere thermal gravity anomaly correction to account for the lithosphere mass deficiency from the elevated geothermal gradient within oceanic and thinned continental margin lithosphere. Failure to include the lithosphere thermal gravity anomaly correction at rifted continental margins leads to predictions of Moho depth and crustal basement thickness which are too great and continental lithosphere thinning factors which are too low. The thermal gravity anomaly correction is dependent on the thermal re-equilibration time since lithosphere stretching and thinning, and therefore on continental breakup age. We have used 110Ma as the age of breakup, after Moulin (2005), for the thermal re-equilibration time to determine the lithosphere thermal gravity anomaly correction, but have also examined sensitivities to ages for thermal re-equilibration which span the period Berriasian (140Ma) to early Albian (110Ma). This range corresponds to the start and end of the main rifting episode in the South Atlantic (Teisserenc and Villemin, 1989). A more detailed description of the gravity anomaly inversion methodology is described in Chappell and Kusznir (2008) and Greenhalgh and Kusznir (2007), whilst the example applications are described in Alvey et al. (2008) and Cowie and Kusznir (2012).

Moho depths determined from the gravity anomaly inversion are in good agreement with those determined from the CS1-2400 seismic reflection profile. Moho depths predicted from gravity anomaly inversion for sensitivities to reference Moho depth are shown in Figure 3(a). The reference Moho depth has been calibrated on the CS1-2400 profile using the clear oceanic Moho reflectors. Calibration (Figure 3(b)) shows that a reference Moho depth of 35.5km is required in order to predict crustal basement thicknesses consistent with those seen in the oceanic domain of the CS1-2400 seismic reflection profile.

A crustal cross section along the CS1-2400 profile (Figure 4(a)) has been constructed using Moho depths predicted from gravity anomaly inversion assuming the calibrated reference Moho depth of 35.5km; bathymetry and 2D sediment thickness are from the CS1-2400 seismic profile. The corresponding continental lithosphere thinning factors (γ) predicted from gravity anomaly inversion, assuming depth uniform stretching and thinning are shown in Figure 4(b). Continental lithosphere thinning factors of zero indicate that there has been no stretching or thinning of the continental lithosphere, whereas a continental lithosphere thinning factor of one indicates that there has been infinite stretching and thinning of the original continental lithosphere and that no continental crust or lithosphere remains.

Stretching of continental lithosphere leads to a decrease in crustal basement thickness; however, decompression melting during rifting and seafloor spreading generates oceanic crust, SDRS (seaward dipping reflectors) and magmatic under plating, which increases crustal basement thickness. A correction for magmatic addition has been included within the gravity anomaly inversion method, and uses a parameterization of the decompression melting model of White and McKenzie (1989) to predict the thickness of the crustal magmatic addition (see Chappell & Kusznir (2008) for a detailed explanation). Sensitivities to magmatic addition including a normal magmatic and a magma poor solution have been examined along the CS1-2400 profile (Figure 4(b)). At the western end of the profile we prefer the normal magmatic solution; however, in the central region of the profile we believe that the magma poor solution is preferential.

Palaeo-bathymetry of the base Aptian salt deposition for the CS1-2400 profile

Flexural backstripping and decompaction has been applied to the CS1-2400 profile (Figure 5(a) to remove the salt and post-salt sedimentary layers in order to determine the bathymetry corrected for sedimentary loading to base salt (Figure 5(b)). Flexural backstripping and decompaction assumes shaly-sand compaction and density parameters (Sclater and Christie, 1980) during the removal of the sedimentary layer, whilst the salt layer is given a simple salt lithology (Hudec and Jackson, 2007) (Table 1).

The complex salt movement in this region may appear to be problematic for flexural backstripping. However, within the palaeo-bathymetric restoration we use the base salt as the target surface for backstripping, which allows us to ignore the salt movement, as we flexurally backstrip through the salt to the time of deposition. We are able to disregard the salt movement because as the salt moved the lithosphere would have responded isostatically to compensate.

The bathymetry corrected for sediment loading and decompaction to base salt (Figure 5(b)) is sensitive to the effective elastic thickness (Te) or lithosphere flexural strength (Bertotti et al., 1998; Galán and Casallas, 2010; Roberts et al., 1998). The effective elastic thickness depends on the bending stresses applied to the plate, the rate of stress application, the lithosphere composition and the geothermal gradient (Kusznir and Karner, 1985). Sensitivities to effective elastic thicknesses of 1.5km, 5km and 10km used in our flexural backstripping have been examined. A finite effective elastic thickness is required for syn-rift flexural backstripping in order to preserve fault block topography (Kusznir et al., 1995; Roberts et al., 1998); the use of Airy (local) isostasy in flexural backstripping (corresponding to Te=0km) produces unrealistic internal deformation of individual fault-blocks. Roberts et al. (1998) showed that effective elastic thicknesses between 1.5km and 5km are required for syn-rift extensional settings in order to match observed fault block geometries and dips. Roberts et al. (1998) showed that relatively long wavelengths loads of post-rift subsidence and sediment loading are relatively insensitive to effective elastic thickness. During the post-rift the lithosphere cools and gets flexurally stronger, therefore, in the post-rift the effective elastic thicknesses will be larger, which act to freeze in the structures and the short wavelength isostatic response from the syn-rift. In this study we therefore use a low effective elastic thickness (Te=1.5km) appropriate for syn-rift flexurally backstripping.

The application of flexural backstripping and decompaction gives an incomplete palaeo-bathymetric restoration of base salt; we also need to include reverse post-breakup thermal subsidence. We determine the magnitude of reverse post-breakup thermal subsidence by the continental lithosphere thinning factor ($\gamma=1-1/\beta$) which we derive from gravity anomaly inversion. Lithosphere thinning factors from gravity inversion are shown in Figure 5(c); sensitivities for a normal magmatic solution and a magma poor solution have been examined. At the western end of the CS1-2400 profile the continental lithosphere thinning factors for a normal magmatic solution are 1.0; whereas for a magma poor solution, the continental lithosphere thinning factors are approximately 0.85. In the central section of the profile, the continental lithosphere thinning factors, for both solutions examined, are between 0.7 and 0.85.

The restored palaeo-bathymetry to base salt, including reverse thermal subsidence modelling, is shown in Figure 5(d) assuming a normal magmatic solution and a breakup age of 112Ma. The proximal base salt restores to just below global sea level with an average bathymetry of approximately 0.3km. In contrast, the distal base salt does not restore to near sea level; restored palaeo-bathymetries for the distal base salt (smoothing through fault controlled topography) are between approximately 0.9km and 2.5km below global sea level. In the deep fault controlled troughs, palaeo-bathymetries for the distal base salt of approximately 4.0km below sea level are predicted.

Assuming a magma poor solution (Figure 5(e)), the restored palaeo-bathymetry to base salt also shows that the proximal base salt restores to just below sea level, whilst the distal base salt again does not. The predicted palaeo-bathymetries of the distal base salt range between approximately 0.9km and 3km below sea level (smoothing through fault controlled topography); in the deep structural troughs the palaeo-bathymetries are greater (approximately 4.5km below sea level).

The lower thinning factors from gravity inversion for the magma poor solution result in less reverse post breakup thermal subsidence and a slightly greater predicted bathymetry for base salt compared with the normal magmatic addition solution. The normal magmatic addition solution (Figure 5(d)) is applicable to the oceanic part of the profile while the magma poor solution (Figure 5(e)) is applicable to the continental end of the profile, with a transitional region in between.

The restoration of base salt palaeo-bathymetry (Figures 5(d) and (e)) using reverse post-breakup thermal subsidence modelling only restores thermal subsidence. It does not restore syn-rift (syn-tectonic) subsidence and the consequences of crustal thinning; subsidence arising from syn-tectonic crust and lithosphere thinning is not included in the restoration.

In the oceanic domain, depths of approximately 2.5km (± 0.2km depending on magmatic solution), consistent with an oceanic ridge are predicted, for both a normal magmatic and a magma poor solution.

An additional sensitivity to the continental lithosphere thinning factors, used to drive reverse thermal subsidence, has been examined for CS1-2400 profile. A continental lithosphere thinning factor of 1.0 (corresponding to $\beta=\infty$), which gives an upper bound of the restored post-breakup thermal subsidence, has been applied to the entire profile (Supplementary Figure S1). The predicted bathymetry for the base of the distal salt remains almost unchanged at between 2km and 3km below global sea level. This implies that, if the base distal salt was deposited at or just below global sea level, it has subsided not only due to post-breakup thermal subsidence and sediment loading.

Due to the thick sedimentary cover and mobile salt (including salt diapirs and canopies), seismic imaging of the salt and pre-salt sedimentary units is difficult, which could lead to errors in our interpretation of the internal structure and thickness of the salt and the pre-salt sedimentary layers. We are however, more confident in our pick of the base salt. In order to understand the implications of either over or under estimating the thickness of the salt layer we have examined the effect of treating the salt layer as a sedimentary layer with a shaly sand lithology within the gravity inversion and in the reverse post-breakup subsidence modelling (Figure 6). The presence of the salt layer effects the decompaction and thinning factor estimates. If there was no salt along the margin, this would result in a deeper Moho (Figure 6(a)) and smaller continental lithosphere thinning factors (Figure 6(b)) from the gravity inversion, which in turn would lead to less reverse modelled thermal subsidence and a deeper restoration of the base salt (Figure 6(c)). The largest differences between the palaeo-bathymetric restorations of the base salt with the salt layer compared to that produced without the salt layer are seen in the large troughs at the western end of the profile (approximately 0.3km difference). The inclusion or omission of the salt layer does not fundamentally change the predicted palaeo-bathymetry of base salt.

Figure 5 (d and e) are calculated using a breakup age within the gravity inversion and reverse thermal post-breakup thermal subsidence modelling of 112Ma. Seismic reflection shows a thick pre-salt sediments up to 8km thick (Unternehr et al., 2010) beneath the proximal salt which almost certainly consists of a lower syn-rift sequence with a sag post-rift sequence above. The rift age in this region is older than breakup and may be as old as 140 Ma (Teisserenc and Villemin, 1989). The effect of using 140 Ma as the rift age (the age for thermal re-equilibration in the gravity inversion and reverse thermal subsidence modelling) gives a slightly deeper base proximal salt palaeo-bathymetry but does not change the overall result that base proximal salt restores to a much shallower palaeo-bathymetry than the distal salt.

In our analysis, we assume depth uniform lithosphere stretching for both the determination of the lithosphere thermal gravity anomaly correction and the reverse post-breakup thermal subsidence modelling and thinning. While the possibility of depth dependent lithosphere stretching and thinning during rifted continental margin formation has been postulated (e.g. Davis and Kusznir (2004)and Kusznir and Karner (2007)), we prefer to assume depth uniform stretching in the absence of reliable fault extension observations.

Reverse post-breakup subsidence for the P3 and P7+11 profiles

In addition to the CS1-2400 profile, we have also applied the reverse post-breakup thermal subsidence modelling to the more northerly P3 and P7+11 profiles (Figures 7 and 8). Results are comparable to those predicted for the CS1-2400 profile; with the proximal base salt restoring to approximately sea level whilst the distal base salt restores to between 2km and 3km below global sea level.

Predicted thinning factors from gravity inversion, assuming normal magmatic addition, are 1.0 at the western end of both P3 and P7+P11 profiles consistent with the presence of oceanic crust. Predicted palaeo-bathymetries for the western end of both profiles are on average 2.85km, consistent with water depths on newly formed oceanic crust. Continental lithosphere thinning factors predicted from gravity inversion under the salt are dependent on whether normal or magma poor decompression melting is assumed. This difference in thinning factor leads to a difference in the predicted bathymetry of base salt from reverse thermal subsidence modelling. Nonetheless, for both profiles, the predicted palaeo-bathymetries for base proximal salt are at or just below global sea level, while the palaeo-bathymetry of base distal salt is between 2km and 3km. At the extreme eastern end of profile P7+11 the predicted sub aerial exposure of approximately 0.9km is probably an edge effect from the flexural backstripping or a decompaction artifact.

Calibration of the reference Moho depth used within the gravity anomaly inversion, for the P3 and P7+11 profiles, gives a reference Moho depth of 37.5km, which is larger than that predicted for the CS1-2400 profile. We have therefore, considered the sensitivity to reference Moho depth within the reverse post-breakup thermal subsidence modelling (Supplementary Figure S2), using CS1-2400 as the example. Increasing the reference Moho depth from 35.5km to 37.5km results in a deeper Moho and smaller continental lithosphere thinning factors predicted from gravity anomaly inversion, and a deeper restoration of the base salt. The largest differences between the palaeo-bathymetric restorations of the base salt for a reference Moho depth of 35.5km compared to that produced with a reference Moho depth of 37.5km are seen in the large troughs at the western end of the profile (approximately 0.35km difference).

Location of the distal salt with respect to COB location along the CS1-2400 profile

Knowledge of the horizontal position of the distal salt with respect to the continent-ocean boundary (COB) and ocean-continent transition (OCT) structure is important for understanding the depositional context of the base Aptian salt and how the salt sits within the broad framework of the OCT. The structure of the OCT and COB location have been investigated using gravity anomaly inversion, sediment corrected residual depth anomaly (RDA) analysis and subsidence analysis. A detailed description of the methodologies of these techniques is beyond the scope of this paper, but is described in Cowie (2015).

The results from these techniques applied to the CS1-2400 profile are shown in Figure 9. We interpret the analysis results as showing three distinct crustal zones along the profile: oceanic crust towards the western end of the profile, hyper-extended continental crust in the centre of the profile, and continental crust at the eastern end of the profile. The dashed lines indicate the boundary between each of these interpreted crustal domains; although these interfaces are shown as a sharp line, in reality they are likely to be transitional boundaries. The COB is identified as the ocean ward start of 'normal' oceanic crust and is identified by changes in crustal basement thickness, inflections in the RDA analysis signal and also changes in the continental lithosphere thinning from subsidence analysis and gravity anomaly inversion.

In the interpreted oceanic domain at the western end of the profile, crustal basement thicknesses (Figure 9(a)) predicted from gravity anomaly inversion are approximately 7km, as expected for oceanic crust. Oceanic crust of normal thickness should have a sediment corrected RDA of approximately zero, notwithstanding the contribution of mantle dynamic topography. The slightly positive sediment corrected RDA in this domain (Figure 9(b)) is consistent with the presence of oceanic crust together with some mantle dynamic uplift, as reported by Crosby & McKenzie (2009) for the Angolan margin. Continental lithosphere thinning factors from gravity anomaly inversion and subsidence analysis (Figure 9(c)) are 1.0, also consistent with the presence of oceanic crust. Between the oceanic domain and the hyper-extended continental crust domain, we see an increase in crustal basement thickness and the RDA signal, whilst the continental lithosphere thinning factors decrease. In our interpreted hyper-extended continental crust domain, gravity anomaly inversion predicted crustal basement thicknesses range between 7km and 12km. The sediment corrected RDA increases before plateauing at approximately 1000m, whilst the continental lithosphere thinning factors decrease from 1.0 to between 0.7 and 0.85, which is indicative of thinned continental crust. At the western end of the hyper-extended continental crust domain, the thinning of the continental crust may increase together with the start of magmatic addition as ocean crust is approached. Our interpretation of the presence of hyper-extended continental crust in this domain is significantly different to that proposed by Unternehr et al. (2010), who proposes the presence of serpentinized exhumed mantle. Our quantitative analysis results show no evidence of exhumed mantle; exhumed mantle would show a thinner crust from gravity inversion, lower (negative) sediment corrected RDAs and higher continental lithosphere thinning factors. At the eastern end of the profile we interpret continental crust as the crustal basement thickness and sediment corrected RDA increases, whilst the continental lithosphere thinning factors decrease to between 0.2 and 0.4.

We have identified the location of the COB on Figure 5, by the dashed line, in order to see where the salt sits within the OCT. We believe that the majority of the salt along the CS1-2400 profile is located to the east of the COB and is underlain by hyper-extended continental crust.

Discussion

Predicted palaeo-bathymetries have been determined for the base Loeme salt using 2D-flexural backstripping and decompaction, together with reverse modelling of post-breakup thermal subsidence. Continental lithosphere thinning factors derived from gravity anomaly inversion have been used to determine the reverse post-breakup thermal subsidence. Sensitivities to normal magmatic and magma poor solutions for determining thinning factors from gravity inversion have been examined. For profile CS1-2400, thinning factors, from both the normal magmatic and magma poor solutions, used to drive the reverse post-rift thermal subsidence modelling restore the proximal autochthonous base salt to between 200m and 300m below global sea level at the time of breakup. A similar palaeo-bathymetry for base proximal salt at breakup is predicted for profile P7-11. For profile P3, predicted base proximal salt palaeo-bathymetry is slightly shallower with values at or just below global sea level. In contrast, for all three profiles, reverse post-breakup subsidence modelling restores the distal base salt to between 2km and 3 km below global sea level Even if we apply a continental lithosphere thinning factor of 1.0 to drive the reverse post-rift thermal subsidence along the full length of the three profiles (which is unreasonable), the palaeo-bathymetries of base distal salt do not restore to sea level, demonstrating that it is not possible to generate the subsidence of the base salt by post-rift subsidence alone. The predicted bathymetries at breakup of the first unequivocal oceanic crust are approximately 2.5km as expected for newly formed oceanic crust of normal thickness. As previously mentioned, sensitivities to effective elastic thickness and breakup age have been examined. The value of effective elastic thickness does not significantly change the palaeo-bathymetry predictions. Changing the breakup age has a small effect on the palaeo-bathymetry predictions but does not change the overall conclusions.

We consider several possible explanations of the palaeo-bathymetric restoration of the distal base salt to water depths substantially below sea level:

(i) All the Aptian salt along the northern Angolan profiles was deposited between 200m and 300m below global sea level, but the distal salt was emplaced during late syn-rift while the continental crust under it was being actively thinned resulting in additional tectonic subsidence. This is consistent with seismic evidence, which shows that the distal base salt is extensionally faulted. Also crustal basement thicknesses from gravity inversion, RDA and subsidence analysis, summarised in Figure 9, suggest that the distal salt is underlain by hyper-extended continental crust rather than oceanic crust or exhumed mantle. In contrast to the distal salt, the proximal salt formed in a region where crustal thinning had already taken place, but had ceased. This interpretation requires that the distal salt subsides by syn-rift crustal thinning and post-rift thermal subsidence, whilst the proximal salt subsides by post-rift thermal subsidence alone. Diachronous thinning of the continental crust from inboard to outboard is to be expected from both observation and modelling ,and is consistent with breakup tectonic models proposed by Péron-Pinvidic and Manatschal (2009), Pindell and Kennan (2007), Ranero & Perez-Gussinye (2010) and Brune et al. (2014).

(ii) An alternative explanation is that during breakup the distal salt moved down-slope to its present position into much deeper water (and is para-autochthonous). If in the distal regions, the salt is para-autochthonous (or allochthonous) this suggests that it was not deposited in deep water and that the salt should not restore to sea level. This interpretation is similar to that advocated in the Gulf of Mexico by Hudec et al. (2013) and Rowan and Vendeville (2006).

(iii) An interpretation which is often invoked (e.g. Burke and Sengör (1988), Burke et al. (2003) and Karner and Gambôa (2007)) to explain the palaeo-bathymetry of the base Aptian salt along the northern Angolan margin is that the Aptian salt deposition occurred in confined environmental conditions (e.g. in a Messinian-type basin, isolated from global sea level). Although a structural barrier in the south is not dismissed, we believe that there is no definite requirement to invoke an isolated ocean basin with local sea level 2km and 3km below global sea level for the deposition of the Aptian salt on the Angolan rifted margin. A strong argument against the isolated basin interpretation is presented by Pindell et al. (2014) , with reference to the Gulf of Mexico. Pindell et al. (2014) argue that an isolated basin hypothesis is unlikely as it requires a complicated scenario of inter-related events to occur. They propose that first rifting must produce a large basin area in which the depositional surface remains approximately 2km below sea level, there must also be land barriers, which are able to block out the global sea during the formation of the large basin. Then, at the time of salt deposition there needs to have been repeated spill/desiccation cycles and a semi-permeable barrier which continuously allowed just the right amount of sea water into basin so that shallow-water evaporative conditions were maintained until the end of the salt deposition.

Our preferred interpretation of our palaeo-bathymetric restoration of the base Aptian salt along the northern Angolan profiles is the first interpretation with a possible contribution from the second interpretation. In summary we believe that both proximal and distal Aptian salt on the Kwanza margin was deposited at a datum 200-300 m below global sea level, but that the distal salt was deposited during late syn-rift while the crust under it was being actively thinned which resulted in additional tectonic subsidence. It is possible that some of the distal salt is para-autochthonous and moved down-slope to its present day position. It is also possible that syn-tectonic (pre-breakup) extension continued post-salt deposition in the distal region.

Figure Captions:

Table 1 – Compaction and density parameters used within the reverse post-breakup thermal subsidence modelling.

Figure 1: Data used in the reverse post-breakup thermal subsidence modelling and gravity anomaly inversion for the northern Angolan rifted continental margin. (a) Bathymetry (km) (Amante and Eakins 2009), with the location of profiles CS1-2400, P3 and P7+11 indicated. (b) Satellite derived free air gravity (mgal) (Sandwell and Smith 2009). (c) Deep long-offset seismic reflection depth section (PSDM) for the ION-GXT CS1-2400 profile. (d) Seismic velocity model along the P3 profile (Contrucci et al., 2004; Moulin et al., 2005) from seismic refraction data. (e) Seismic velocity model along the P7+11 profile (Contrucci et al., 2004; Moulin et al., 2005) from seismic refraction data.

Figure 2: Schematic series of sequential cross sections showing reverse post-rift thermal subsidence modelling from present day to base post-rift for a hypothetical rift basin (Kusznir et al., 1995).

Figure 3: Calibration of the reference Moho depth used in the gravity anomaly inversion against seismic Moho depths for the CS1-2400 profile on the northern Angolan margin. (a) Sensitivity of Moho depth predicted from gravity anomaly inversion to reference Moho depths of 32.5km, 35km and 37.5km. (b) Cross-plot of ΔZMoho (the difference between the gravity inversion predicted Moho depth and seismic Moho depth) against the value of reference Moho depth used in the gravity inversion. Calibration gives a reference Moho depth of 35.5km.

Figure 4: (a) Crustal cross section along the CS1-2400 profile, showing Moho depth from gravity anomaly inversion, using the calibrated reference Moho depth of 35.5km. (b) Continental lithosphere thinning profile, predicted from gravity anomaly inversion, along the CS1-2400 profile. Sensitivities to a normal magmatic solution and a magma poor solution have been examined. A normal magmatic solution predicts thinning factors of 1.0 at the western end of the profile and a

magma poor solution predicts continental lithosphere thinning factors of approximately 0.85 in this region.

Figure 5: Flexural backstripping and reverse post-breakup thermal subsidence modelling along the ION-GXT CS1-2400 profile. (a) Digitized present day cross section along the CS1-2400 profile; the post-salt sedimentary layer is highlighted in blue; pre-salt sedimentary layer in pink; the salt layer is highlighted in yellow; crust is grey and mantle is red. (b) Sediment corrected bathymetry to base salt calculated from flexural backstripping and decompaction, using a Te of 1.5km. (c) Continental lithosphere thinning factor profile, from gravity anomaly inversion, for normal magmatic and magma poor solutions. (d) Reverse post-breakup thermal subsidence modelling along the CS1-2400 profile, assuming a normal magmatic solution. (e) Reverse post-breakup thermal subsidence modelling along the CS1-2400 profile, assuming a magma poor solution.

Figure 6: Summary of the integrated quantitative analysis results for the CS1-2400 profile used to determine OCT structure and COB location. (a) Crustal cross section along CS1-2400 profile with Moho depth from gravity anomaly inversion. (b) The sediment corrected RDA and the RDA component from variations in crustal basement thickness both have the same general trend along the profile although the magnitudes differ. This difference gives an indication of the magnitude of residual topography in this region, which we calculate to be approximately +700m of uplift. (c) Comparison of continental lithosphere thinning factors determined using subsidence analysis and gravity anomaly inversion assuming a normal magmatic solution show the same general trend along profile. The dashed lines on the crustal cross section, RDA and continental lithosphere thinning plots indicate the distal extent of unequivocal continental crust and its boundary with oceanic crust, which is a possible interpretation of the COB.

Figure 7: Flexural backstripping and reverse post-breakup thermal subsidence modelling along the P3 profile (Contrucci et al., 2004; Moulin et al., 2005). (a) Digitized present day cross section along

the P3 profile; the post-salt sedimentary layers are highlighted in turquoise, orange, green and blue; pre-salt sedimentary layer in pink; the salt layer is highlighted in yellow; crust is grey and mantle is red. (b) Sediment corrected bathymetry to base salt calculated from flexural backstripping and decompaction, using a Te of 1.5km. (c) Continental lithosphere thinning factors from gravity anomaly inversion for a normal magmatic and a magma poor solution. (d) Reverse post-breakup thermal subsidence modelling along the P3 profile, assuming a normal magmatic solution. (e) Reverse post-breakup thermal subsidence modelling along the P3 profile, assuming a magma poor solution.

Figure 8: Flexural backstripping and reverse post-breakup thermal subsidence modelling along the P7+11 profile (Contrucci et al., 2004; Moulin et al., 2005). (a) Digitized present day cross section along the P3 profile; the post-salt sedimentary layers are highlighted in turquoise, orange, green and blue; pre-salt sedimentary layer in pink; the salt layer is highlighted in yellow; crust is grey and mantle is red. (b) Sediment corrected bathymetry to base salt calculated from flexural backstripping and decompaction using a Te of 1.5km. (c) Continental lithosphere thinning factors from gravity anomaly inversion for a normal magmatic and a magma poor solution. (d) Reverse post-breakup thermal subsidence modelling along the P7+11 profile, assuming a normal magmatic solution. (e) Reverse post-breakup thermal subsidence modelling along the P7+11 profile, assuming a magma poor solution.

Supplementary Figure S1: Sensitivity to the effect of over-estimating or under-estimating the thickness of the salt layer along CS1-2400. Two end member sensitivities have been considered: (i) having a salt layer (as used in the paper) (labelled “With Salt”) or (ii) treating the salt as just another sedimentary layer (labelled “No Salt”). (a) Crustal cross section from gravity anomaly inversion, showing two Moho depths (both using the calibrated reference Moho depth of 35.5km). The Moho in black is the result of having a salt layer in the gravity anomaly inversion, whereas the Moho in blue is the result of treating the salt layer as just another sedimentary layer. Removing the salt layer from the gravity anomaly inversion results in a deeper Moho depth prediction. (b) Comparison of the continental lithosphere thinning factors, predicted form gravity anomaly inversion for the two sensitivities: with salt (in blue) and no salt (in green). Removing the salt layer from the gravity anomaly inversion results in smaller continental lithosphere thinning factors. (c) The resulting palaeo-bathymetries from reverse post-breakup thermal subsidence modelling for the two sensitivities: with salt (in blue) and no salt (in orange). The “No Salt” sensitivity results in deeper palaeo-bathymetries, the biggest differences are observed in the central section of the profile.

Supplementary Figure S2: Sensitivity to changing the reference Moho depth between 35.5km (as calibrated for the CS1-2400 profile) to 37.5km (as calibrated for the P3 and P7+11 profiles). (a) Crustal cross section from gravity anomaly inversion, showing two Moho depths. The Moho in black is the result of using a reference Moho depth of 35.5km and the Moho in purple is the result of using a higher reference Moho depth of 37.5km. If we increase the reference Moho depth along the CS1-2400 profile, this results in a deeper Moho depth prediction. (b) Comparison of the continental lithosphere thinning factors, predicted form gravity anomaly inversion for the sensitivities to reference Moho depth. Using a reference Moho depth of 37.5km (in red) results in smaller continental lithosphere thinning factors along the CS1-2400 profile. (c) The resulting palaeo-bathymetries from reverse post-breakup thermal subsidence modelling for the two sensitivities to reference Moho depth: using a reference Moho depth of 35.5km (in blue) and using a reference Moho depth of 37.5km (in green). The larger reference Moho depth of 37.5km results in deeper palaeo-bathymetries; the biggest differences are observed in the central section of the profile.

References:

Alvey, A., Gaina, C., Kusznir, N. J., and Torsvik, T. H., 2008, Integrated crustal thickness mapping and plate reconstructions for the high Arctic: Earth and Planetary Science Letters, v. 274, no. 3-4, p. 310-321.

Amante, C., and Eakins, B. W., 2009, ETOPO1 1 Arc-Minute Global Relief Model: Procedures, Data Sources and Analysis: NOAA Technical Memorandum NESDIS NGDC-24, p. 19.

Bertotti, G., Picotti, V., and Cloetingh, S., 1998, Lithospheric weakening during “retroforeland” basin formation: Tectonic evolution of the central South Alpine foredeep: Tectonics, v. 17, no. 1, p. 131-142.

Burke, K., MacGregor, D. S., and Cameron, N. R., 2003, Africa’s petroleum systems: four tectonic ‘Aces’ in the past 600 million years: Geological Society, London, Special Publications, v. 207, no. 1, p. 21-60.

Burke, K., and Sengör, A. M. C., 1988, Ten metre global sea-level change associated with South Atlantic Aptian salt deposition: Marine Geology, v. 83, no. 1–4, p. 309-312.

Chappell, A. R., and Kusznir, N. J., 2008, Three-dimensional gravity inversion for Moho depth at rifted continental margins incorporating a lithosphere thermal gravity anomaly correction: Geophysical Journal International, v. 174, no. 1, p. 1-13.

Contrucci, I., Matias, L., Moulin, M., Géli, L., Klingelhofer, F., Nouzé, H., Aslanian, D., Olivet, J.-L., Réhault, J.-P., and Sibuet, J.-C., 2004, Deep structure of the West African continental margin (Congo, Zaïre, Angola), between 5°S and 8°S, from reflection/refraction seismics and gravity data: Geophysical Journal International, v. 158, no. 2, p. 529-553.

Cowie, L., 2015, Determination of Ocean Continent Transition Structure, Continent Ocean Boundary Location and Magmatic Type at Rifted Continental Margins [PhD: University of Lierpool, 280 p.

Cowie, L., and Kusznir, N., 2012, Mapping crustal thickness and oceanic lithosphere distribution in the Eastern Mediterranean using gravity inversion: Petroleum Geoscience, v. 18, no. 4, p. 373-380.

Crosby, A. G., and McKenzie, D., 2009, An analysis of young ocean depth, gravity and global residual topography: Geophysical Journal International, v. 178, no. 3, p. 1198-1219.

Davis, M., and Kusznir, N., 2004, Depth Dependant lithospheric Stretching at Rifted Continental Margins, *in* Karner, G. D., Taylor, B., Driscoll, N. W., and Kohlstedt, D. L., eds., Rheology and Deformation of the Lithosphere at Continental Margins, Columbia University Press, p. 408.

Galán, R. A., and Casallas, I. F., 2010, DETERMINATION OF EFFECTIVE ELASTIC THICKNESS OF THE COLOMBIAN ANDES USING SATELLITE-DERIVED GRAVITY DATA: Earth Sciences Research Journal, v. 14, p. 7-16.

Greenhalgh, E. E., and Kusznir, N. J., 2007, Evidence for thin oceanic crust on the extinct Aegir Ridge, Norwegian Basin, NE Atlantic derived from satellite gravity inversion: Geophysical Research Letters, v. 34, no. 6, p. L06305.

Hudec, M. R., and Jackson, M. P. A., 2007, Terra infirma: Understanding salt tectonics: Earth-Science Reviews, v. 82, no. 1–2, p. 1-28.

Hudec, M. R., Norton, I. O., Jackson, M. P. A., and Peel, F. J., 2013, Jurassic Evolution of the Gulf of Mexico Salt Basin: AAPG Bulletin, v. 97, no. 1, p. 1683 - 1710.

Jackson, M. P. A., Cramez, C., and Fonck, J.-M., 2000, Role of subaerial volcanic rocks and mantle plumes in creation of South Atlantic margins: implications for salt tectonics and source rocks: Marine and Petroleum Geology, v. 17, no. 4, p. 477-498.

Karner, G. D., and Driscoll, N. W., 1999, Tectonic and stratigraphic development of the West African and eastern Brazilian Margins: insights from quantitative basin modelling: Geological Society, London, Special Publications, v. 153, no. 1, p. 11-40.

Karner, G. D., Driscoll, N. W., and Barker, D. H. N., 2003, Syn-rift regional subsidence across the West African continental margin: the role of lower plate ductile extension: Geological Society, London, Special Publications, v. 207, no. 1, p. 105-129.

Karner, G. D., Driscoll, N. W., McGinnis, J. P., Brumbaugh, W. D., and Cameron, N. R., 1997, Tectonic significance of syn-rift sediment packages across the Gabon-Cabinda continental margin: Marine and Petroleum Geology, v. 14, no. (7-8), p. 973-1000.

Karner, G. D., and Gambôa, L. A. P., 2007, Timing and origin of the South Atlantic pre-salt sag basins and their capping evaporites: Geological Society, London, Special Publications, v. 285, no. 1, p. 15-35.

Kusznir, N., and Karner, G., 1985, Dependence of the flexural rigidity of the continental lithosphere on rheology and temperature: Nature, v. 316, no. 6024, p. 138-142.

Kusznir, N. J., and Karner, G. D., 2007, Continental lithospheric thinning and breakup in response to upwelling divergent mantle flow: application to the Woodlark, Newfoundland and Iberia margins: Geological Society, London, Special Publications, v. 282, no. 1, p. 389-419.

Kusznir, N. J., Roberts, A. M., and Morley, C. K., 1995, Forward and reverse modelling of rift basin formation: Geological Society, London, Special Publications, v. 80, no. 1, p. 33-56.

McKenzie, D., 1978, Some Remarks on the Development of Sedimentary Basins Earth and Planetary Science Letters, v. 40, p. 25-32.

Moulin, M., 2003, Etude géologique et géophysique des marges continentales passives: exemple du Zaıre et de l'Angola [PhD: University de Bretagne Occidentale, 360 p.

Moulin, M., Aslanian, D., Olivet, J.-L., Contrucci, I., Matias, L., Géli, L., Klingelhoefer, F., Nouzé, H., Réhault, J.-P., and Unternehr, P., 2005, Geological constraints on the evolution of the Angolan margin based on reflection and refraction seismic data (ZaïAngo project): Geophysical Journal International, v. 162, no. 3, p. 793-810.

Müller, R. D., Roest, W. R., Royer, J.-Y., Gahagan, L. M., and Sclater, J. G., 1997, Digital isochrons of the world's ocean floor: Journal of Geophysical Research, v. 102, no. B2, p. 3211-3214.

Nurullina, R., 2006, Angola margin : regional tectonic evolution based on integrated analysis of seismic reflection and potential field data and modelling [Master: University of Oslo.

Parker, R. L., 1972, The Rapid Calculation of Potential Anomalies: Geophysical Journal of the Royal Astronomical Society, v. 31, no. 4, p. 447-455.

Péron-Pinvidic, G., and Manatschal, G., 2009, The final rifting evolution at deep magma-poor passive margins from Iberia-Newfoundland: a new point of view: International Journal of Earth Sciences, v. 98, no. 7, p. 1581-1597.

Pindell, J., Graham, R., and Horn, B., 2014, Rapid outer marginal collapse at the rift to drift transition of passive margin evolution, with a Gulf of Mexico case study: Basin Research, p. n/a-n/a.

Pindell, J. L., and Kennan, L., 2007, Rift models and the salt-cored marginal wedge in the norhten Gulf of Mexico: implications for dep water paleogene Wilcox deposition and basinwide maturation: Transactions of GCSSEPM 27th Annual Bob F. Perkins Research Conference, p. 146-186.

Roberts, A. M., Corfield, R. I., Kusznir, N. J., Matthews, S. J., Hansen, E.-K., and Hooper, R. J., 2009, Mapping palaeostructure and palaeobathymetry along the Norwegian Atlantic continental margin: Møre and Vøring basins: Petroleum Geoscience, v. 15, no. 1, p. 27-43.

Roberts, A. M., Kusznir, N. J., Yielding, G., and Styles, P., 1998, 2D flexural backstripping of extensional basins; the need for a sideways glance: Petroleum Geoscience, v. 4, no. 4, p. 327-338.

Rowan, M. G., and Vendeville, B. C., 2006, Foldbelts with early salt withdrawal and diapirism: Physical model and examples from the northern Gulf of Mexico and the Flinders Ranges, Australia: Marine and Petroleum Geology, v. 23, no. 9–10, p. 871-891.

Sandwell, D. T., and Smith, W. H. F., 2009, Global marine gravity from retracked Geosat and ERS-1 altimetry: Ridge segmentation versus spreading rate: J. Geophys. Res., v. B01411, no. 114(B1).

Sclater, J. G., and Christie, P. A. F., 1980, Continental stretching: An explanation of the Post-Mid-Cretaceous subsidence of the central North Sea Basin: Journal of Geophysical Research: Solid Earth, v. 85, no. B7, p. 3711-3739.

Teisserenc, P., and Villemin, J., 1989, Sedimentary basin of Gabon – geology and oil systems, *in* Edwards, J. D., and Santogrossi, P. A., eds., Divergent / Passive Margin Basins. Memoir of the American Association of Petroleum Geologists, Volume 48.

Unternehr, P., Péron-Pinvidic, G., Manatschal, G., and Sutra, E., 2010, Hyper-extended crust in the South Atlantic: in search of a model: Petroleum Geoscience, v. 16, no. 3, p. 207-215.

White, R., and McKenzie, D., 1989, Magmatism at Rift Zones: The Generation of Volcanic Continental Margins and Flood Basalts: Journal of Geophysical Research, v. 94, no. B6, p. 7685-7729.

Layer	Lithology	Porosity	Compaction Coefficient (km^{-1})	Density (kgm^{-3})
Post Salt	Shaly-Sand	63	0.51	2720
Salt	Salt	0	0	2200
Pre-salt	Shaly-Sand	63	0.51	2720

Figure 1

Cowie, Angelo, Kusznir & Manatschal 2014

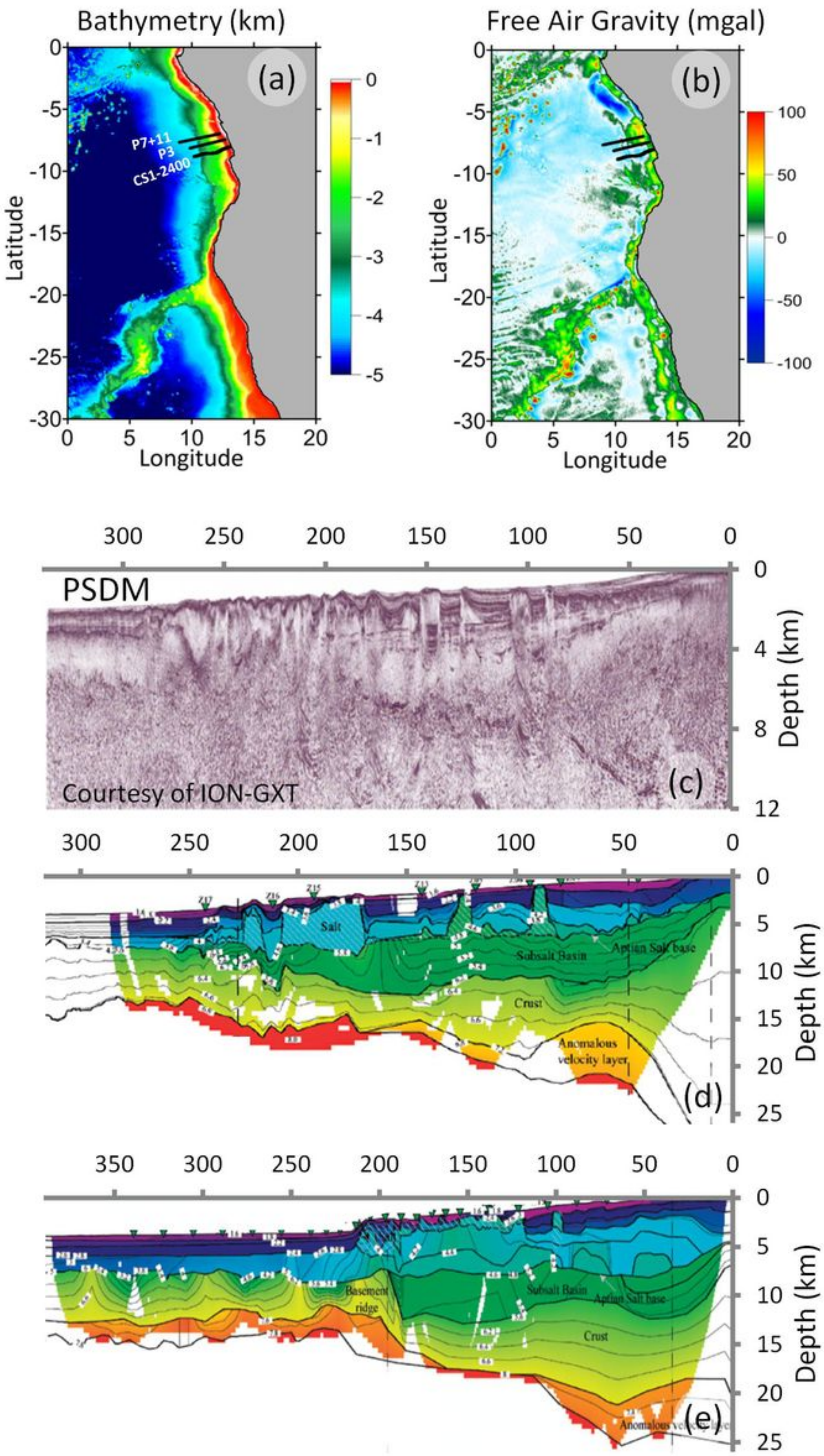

Figure 2

Cowie, Angelo, Kusznir & Manatschal 2014

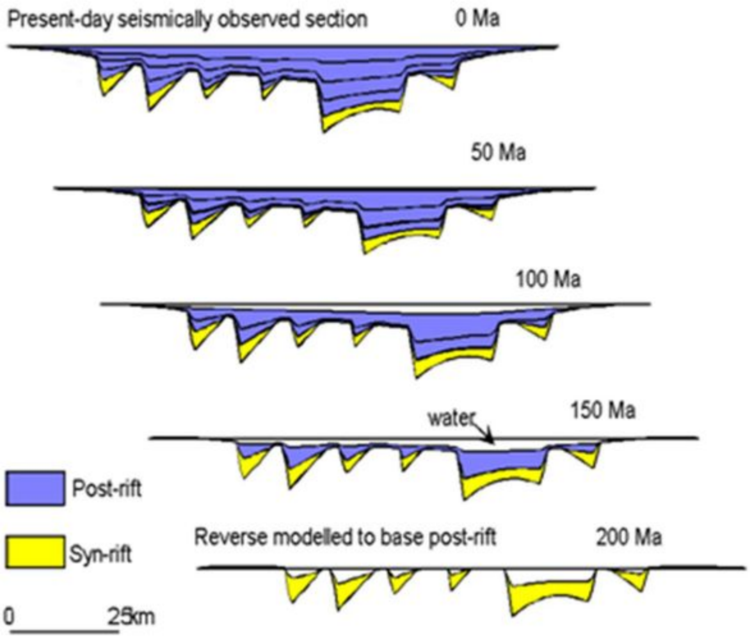

Figure 3

Cowie, Angelo, Kusznir & Manatschal 2014

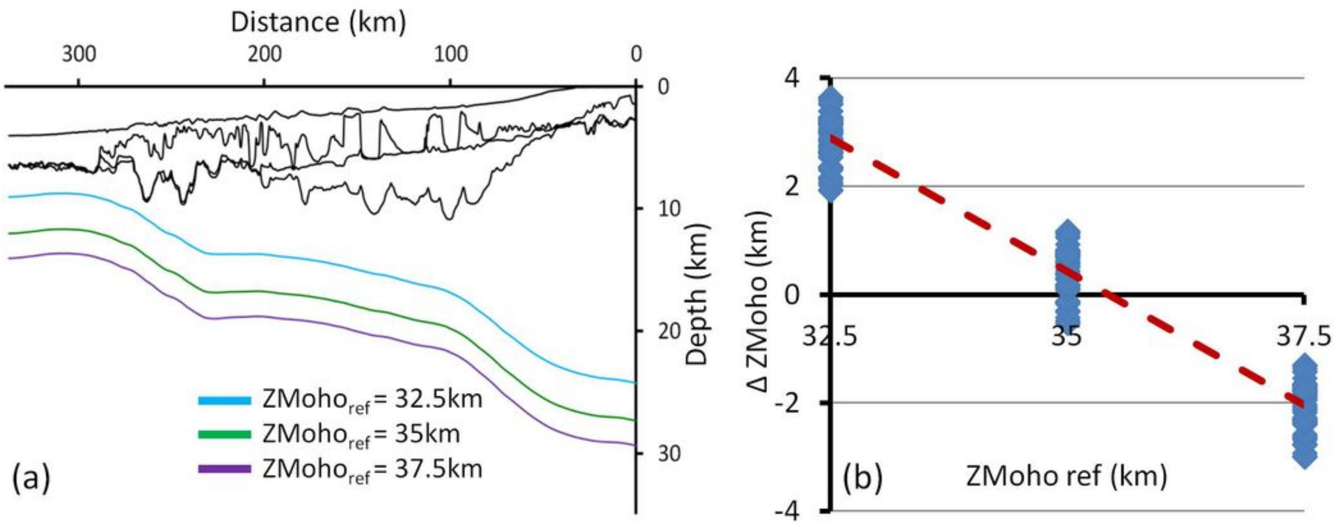

Figure 4

Cowie, Angelo, Kusznir & Manatschal 2014

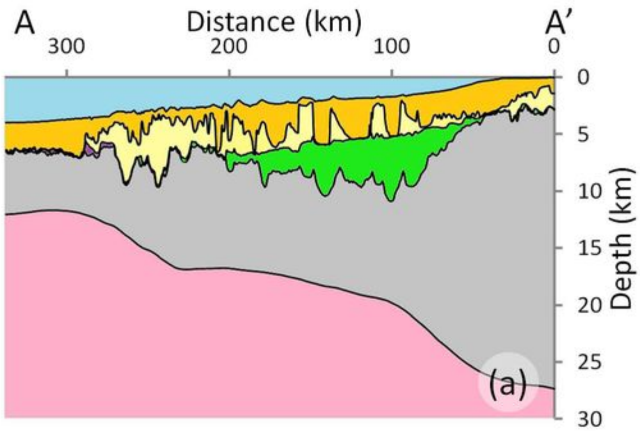

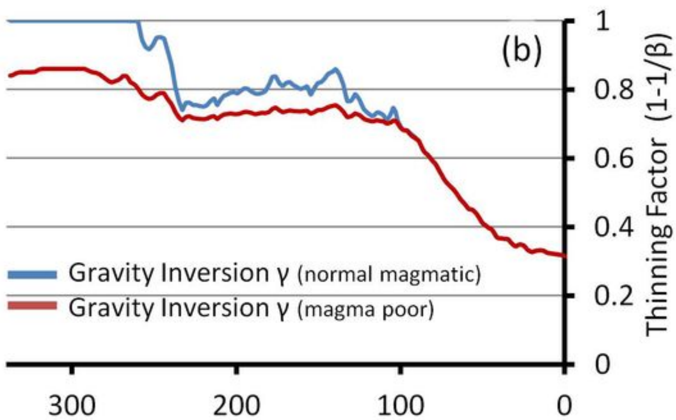

Figure 5

Cowie, Angelo, Kusznir & Manatschal 2014

ION-GXT CS1-2400 profile:

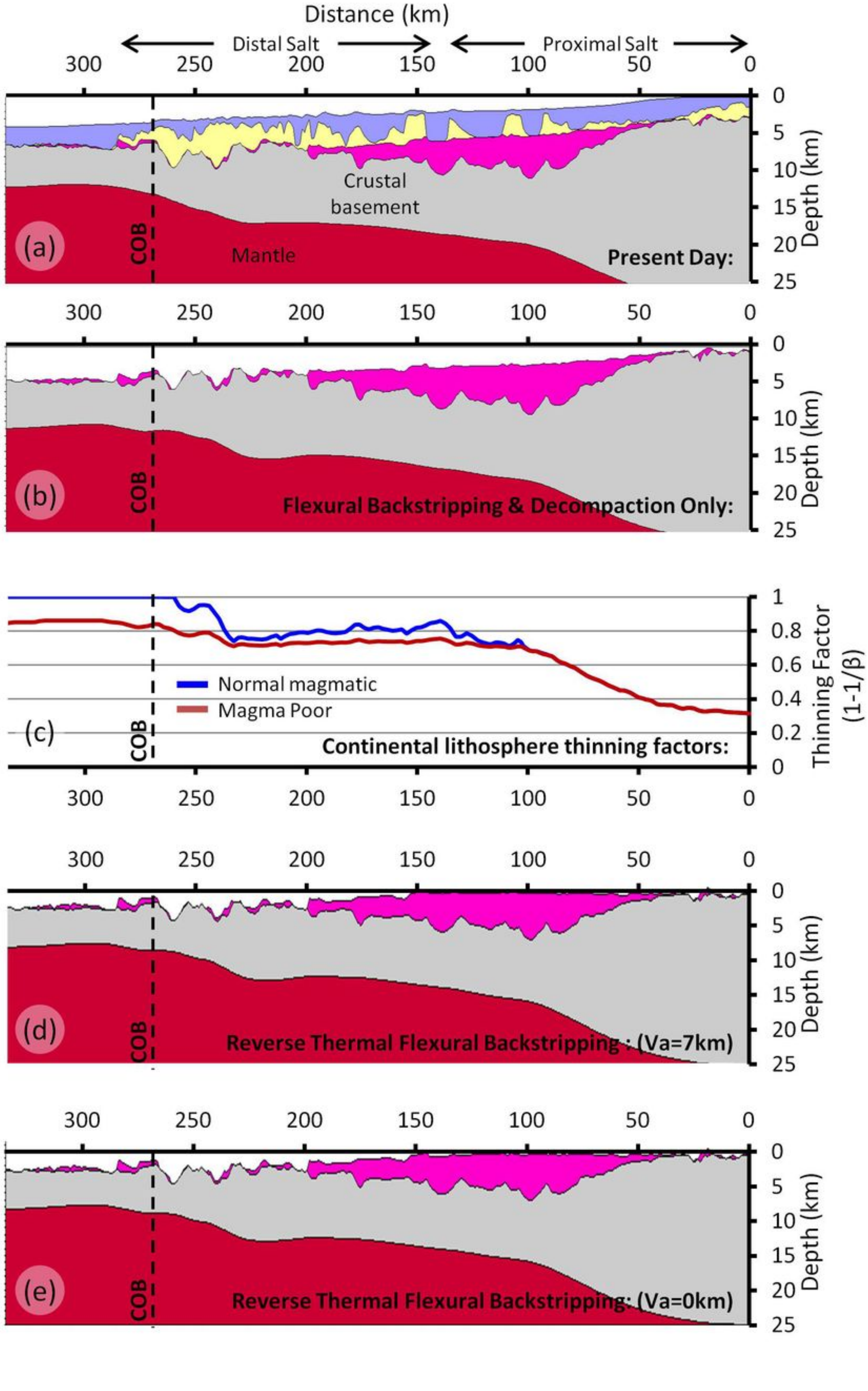

Figure 6

Cowie, Angelo, Kusznir & Manatschal 2014

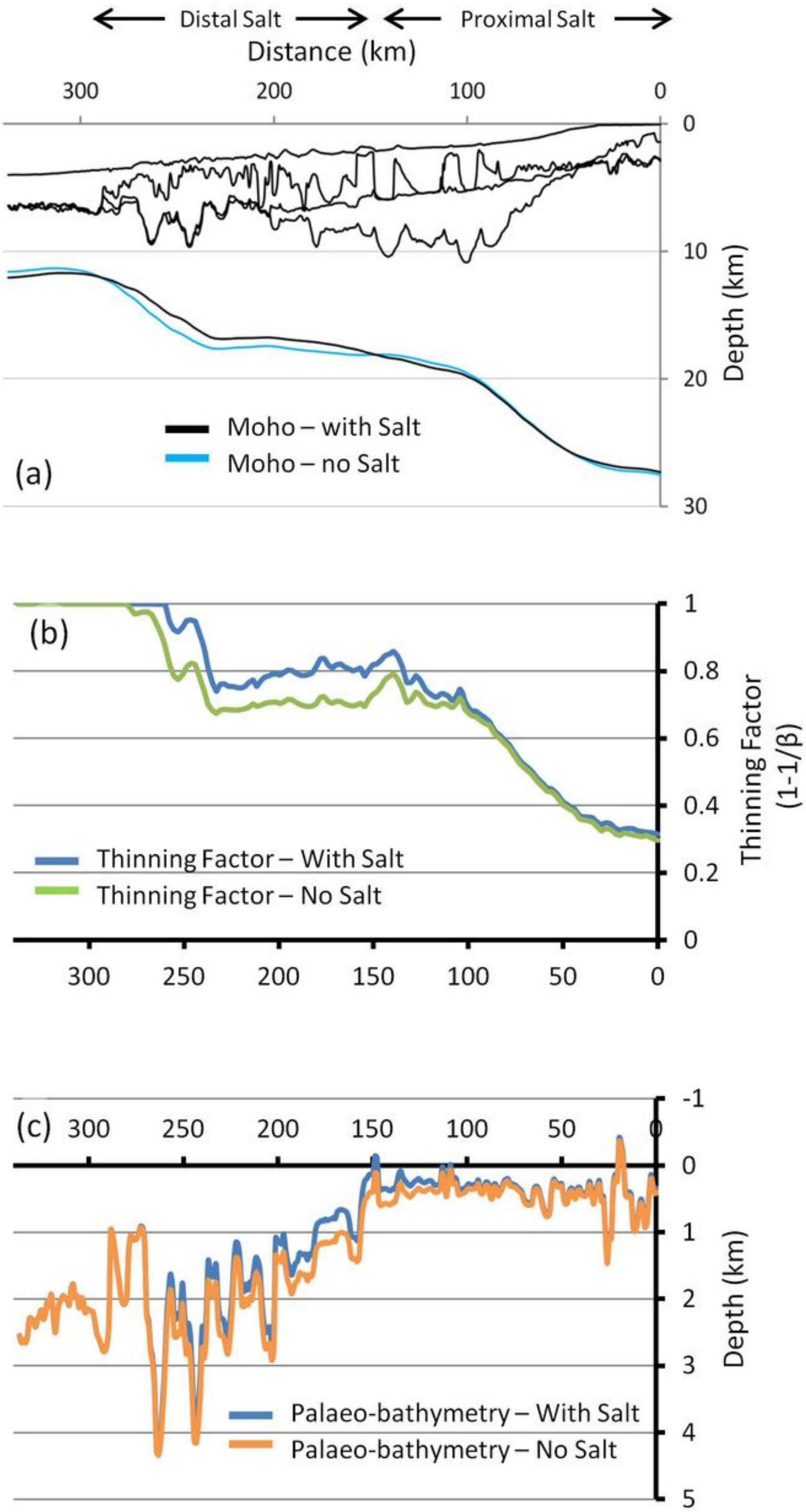

Figure 7
Cowie, Angelo, Kusznir & Manatschal 2014

P3 profile: (Moulin (2003) & Contrucci et al., (2004))

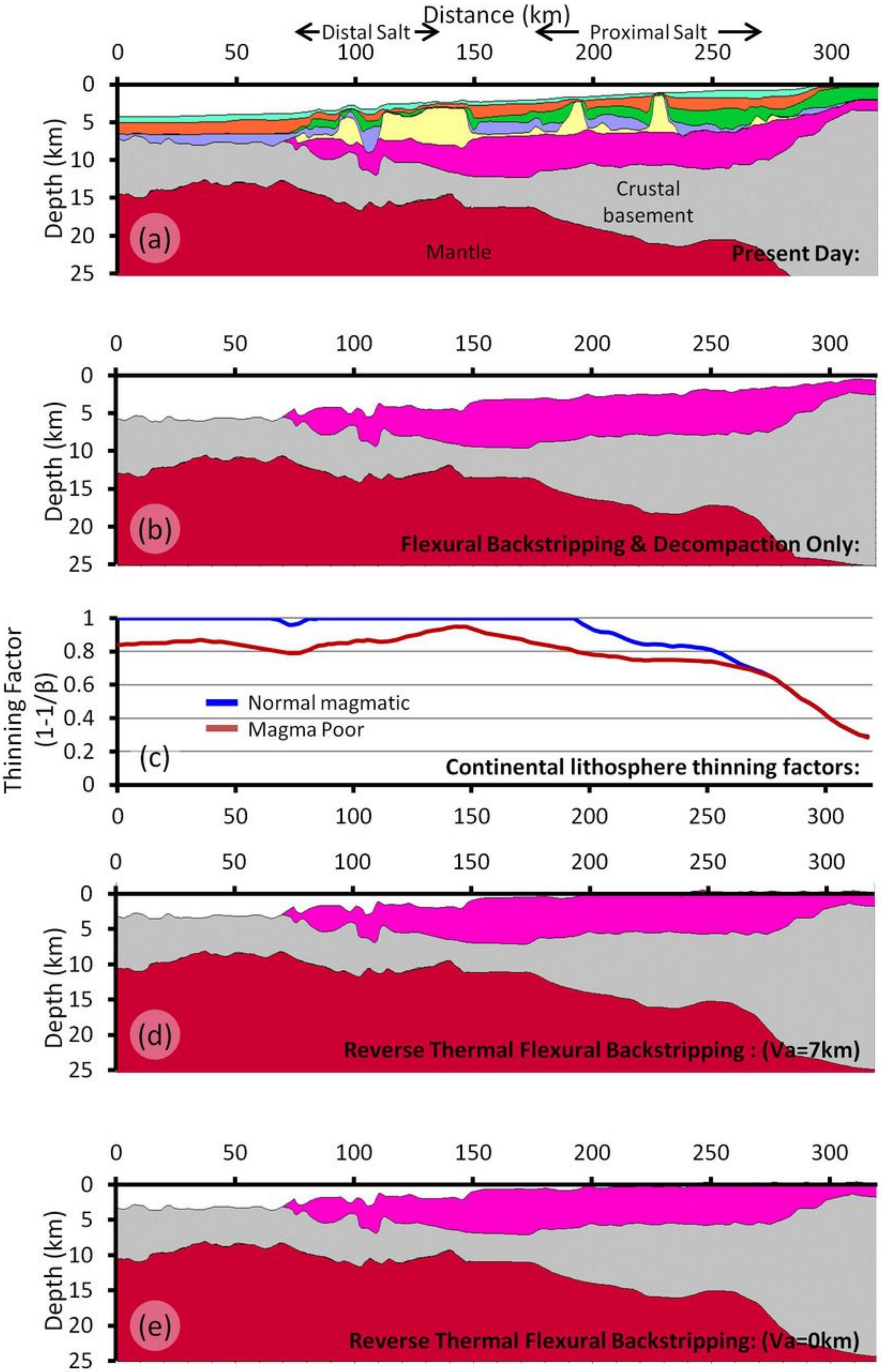

Figure 8

Cowie, Angelo, Kusznir & Manatschal 2014

P7+11 profile (Moulin (2003) & Contrucci et al., (2004))

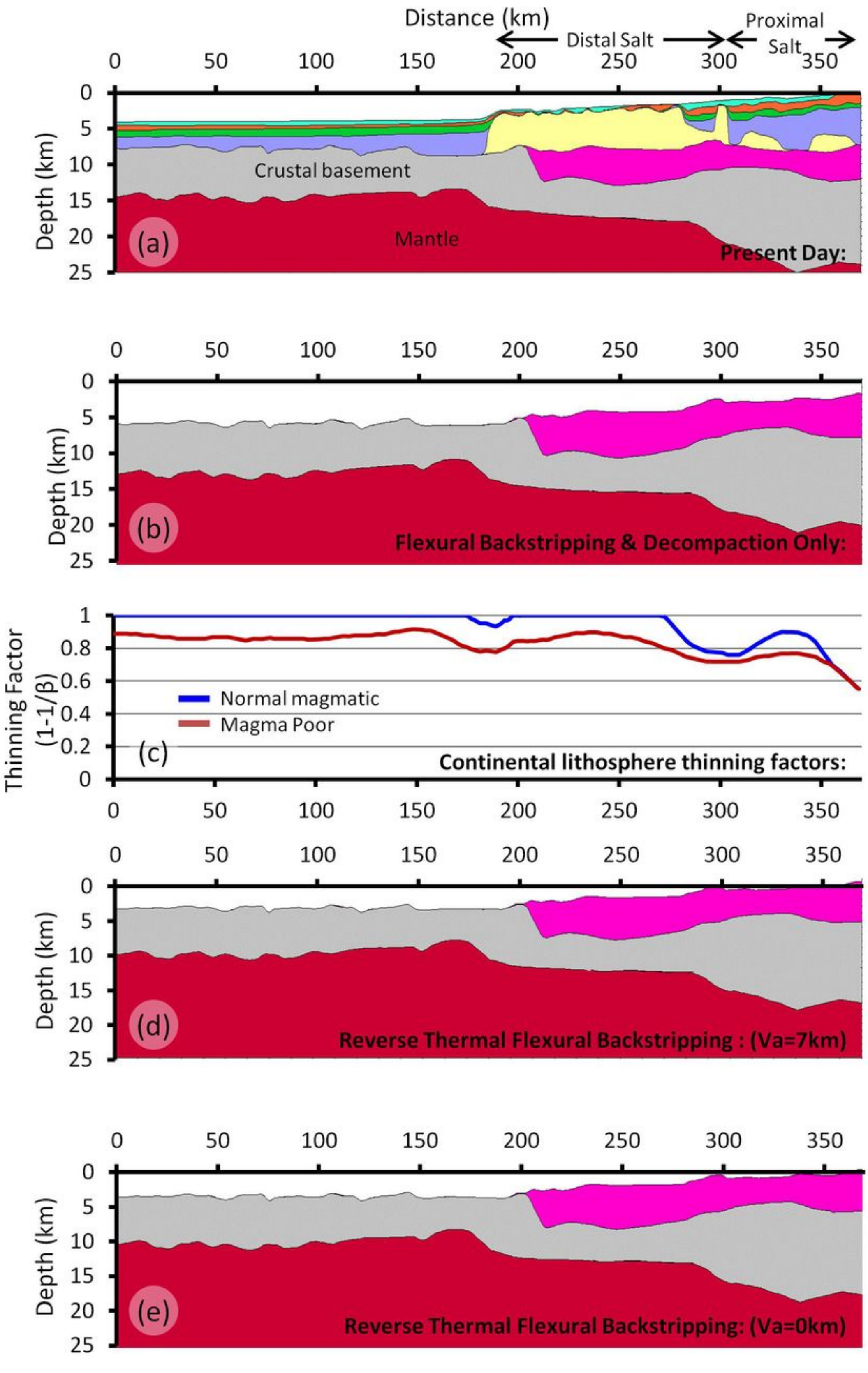

Figure 9

Cowie, Angelo, Kusznir & Manatschal 2014

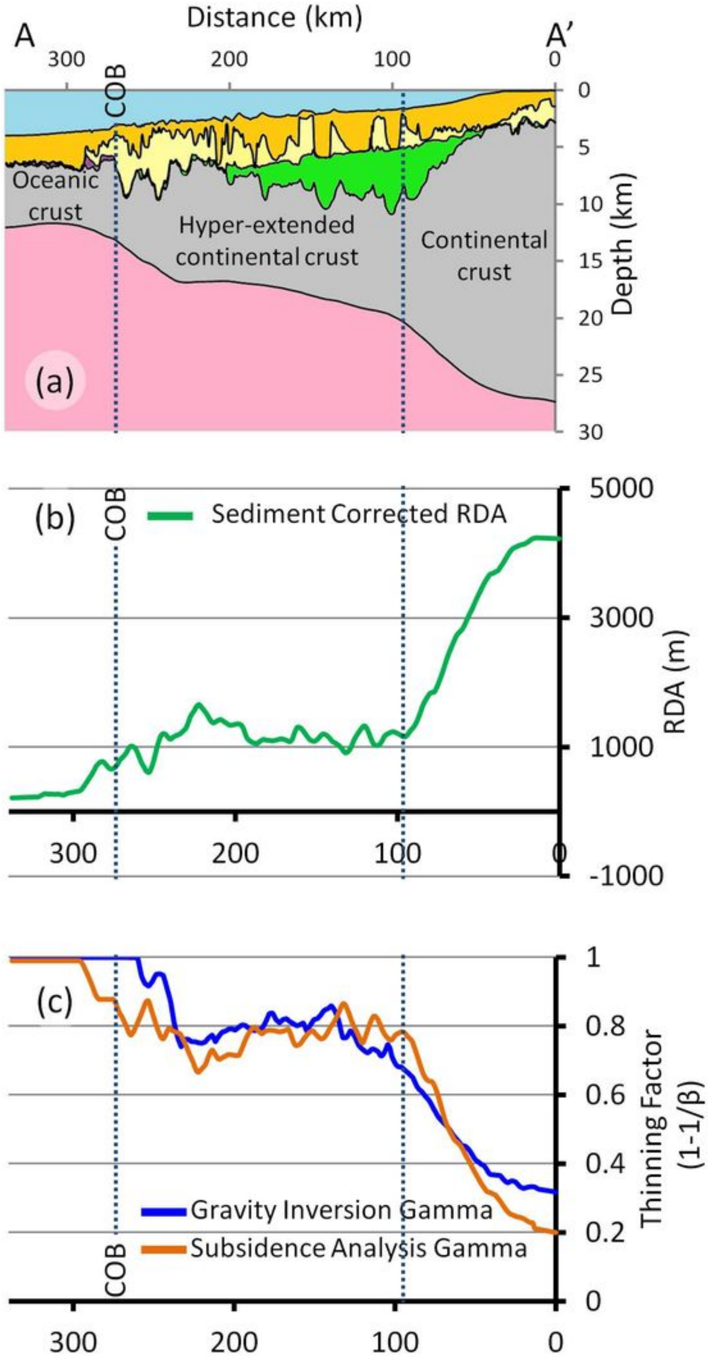

Supplementary Figure 1

Cowie, Angelo, Kusznir & Manatschal 2014

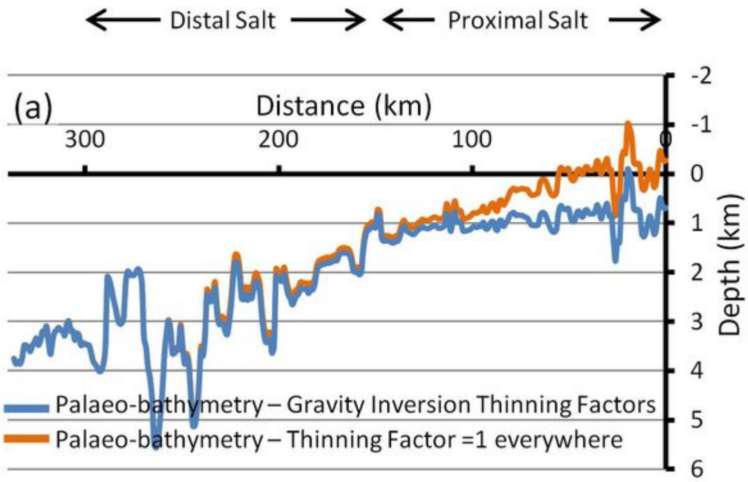

Supplementary Figure 2

Cowie, Angelo, Kusznir & Manatschal 2014